Acoustics 2019
Sound Decisions: Moving forward with Acoustics

An improved correlation of bubble size distribution with the measured acoustic spectrum of a turbulent bubble plume

Li Chen

Maritime Division, Defence Science and Technology, 506 Lorimer Street, Fishermans Bend, VIC 3207, Australia

ABSTRACT

Bubble size distribution is of great interest in many engineering applications. Measuring this quantity in a turbulent bubble plume presents a challenge to conventional techniques, such as photography and ultrasonic imaging. This paper presents an improved correlation of bubble size distribution in turbulent bubble plumes with the measured sound spectrum. The improved correlation includes both the effect of sound attenuation through the bubble plume and the effect of the formed bubble sizes on the magnitude of the generated sound. An iterative method is also used in the solution process. The model is applied to highly turbulent bubble plumes generated at different facilities. It has been found that the total flow rates predicted by using the improved correlation agree well with the measured data and confirm that the magnitude of bubble formation sound is indeed dependent upon the flow conditions.

1 INTRODUCTION

The release of gas into water can be found in many industrial applications. This process results in the formation of bubbles and emits sound. Both the bubble size distribution and bubble generation rate have an important impact on design outcomes. Examples include bubble-mediated medical diagnostics, bubbles related to the stealth of naval platforms, and the contribution of bubbles to ocean background noise. Measuring the bubble generation in a turbulent bubbly plume presents a challenge to conventional techniques, such as photography and ultrasonic imaging. For a dispersed bubble flow, the widely used techniques are optically based such as with PIV and high-speed cameras. Acoustic techniques have shown some promise (Brooks et al. 2009, Berges et al. 2015, Chen et al. 2017 and Chen et al. 2016). A passive acoustic technique inverts the measured acoustic emission from bubble formation to estimate the bubble generation rate and its size distribution. An active acoustic technique inverts the measured sound attenuation to determine the bubble number and size distributions.

Research, usually at low injection rates where the sound from each individual bubble can be identified, has explored the underlying physics both experimentally and theoretically (Cavugab et al. 1956, Leighton and Walton 1987, Deane and Stokes 2008 and Pandit et al. 1992). Recent examples of the use of an acoustic technique to measure volume flow rate can be found in Leblond et al. (2014) and Bok and Suk (2001). Those applications are mainly for low gas-flow rates in which the induced turbulence is low and, as may be expected, the bubble-bubble interaction is weak. However, very often there is a requirement to characterise a turbulent bubble plume for both size distribution and bubble generation rate. When the gas flow rate is high, the bubble plume becomes turbulent and the bubble populations are high. The resulting turbulent gas-liquid flow and high bubble population influence not only the bubble formation dynamics, leading to the deviation of the amplitude of the emitted sound from the ideal situation (Chen et al. 2015 and 2016), but also the sound transmission through it (Deane and Stokes 2010). The accuracy of the estimated distributions will be also reduced by experimental factors which depart from the assumptions of the inversion, such as when absorption, scattering and reverberation are not sufficiently taken into account. Most models assume a free-field and a bubble-free propagation path, and few correct for such features when estimating bubble population using acoustic inversion. Using the passive acoustic technique for characterising the bubble generation and size distribution of a turbulent bubble plume therefore requires proper consideration of those factors. Our earlier model (Chen et. al 2016 and 2017) based on Leighton and White (2011) has taken the effect of gas flow rate on bubble formation dynamics into consideration, but the influence of a potentially high bubble population on the sound transmission has been ignored.

This paper presents an improved correlation of bubble size distribution in turbulent bubble plumes with the measured sound spectrum. The improved correlation includes both the effect of sound attenuation through the bubble plume and the effect of the bubble sizes on the magnitude of the generated sound. The predicted bubble generation rates are compared with the experimental data.

2 THEORY

Consider a bubble plumeand assume that the oscillation of each bubble is not correlated to the motion of surrounding bubbles. In such conditions, the monopole sound emissions,$P(t,R_0)$, of individual bubbles are then uncorrelated. If the bubble generation rate, $D(R_0)$, of bubbles of radius R_0 in the bubble plume is specified, the power spectral density $S(\omega)$ of the sound generated in the far-field and bubble-free medium can be calculated by using:

$$S(\omega) = \int_0^\infty D(R_0)|P(\omega, R_0)|^2 dR_0, \tag{1}$$

If the range of bubble radii are divided into N bands, the bubble generation rate over band n, $\varphi(R_{0,n})$, and the bubble number distribution, $\Psi(R_0)$, are defined as

$$\varphi(R_{0,n}) = \int_{R_{l,n}}^{R_{u,n}} D(R_0)\, dR_0, \text{ and } \Psi(R_0) \approx \sum_{n=1}^{N} \varphi(R_{0,n}), \tag{2}$$

then

$$\Psi(R_0) = S(\omega)\left\{\left|P(\omega, R_{0,n})\right|^2\right\}^{-1}. \tag{3}$$

The spectrum matrix $\left|P(\omega, R_{0,n})\right|^2$ is the squared magnitude of the Fourier transform of the bubble formation sound that is determined by the properties of the gas-liquid mixture (liquid viscosity μ and density ρ) and the gas discharge flow rate Q as

$$\left|P(\omega, R_{0,n})\right|^2 = f(\omega, \rho, \mu, Q) = C(Q)\left|P(\omega, R_{0,n})\right|_{Lw}^2. \tag{4}$$

$\left|P(\omega, R_{0,n})\right|_{Lw}^2$ is the orginal model of Leighton and White (2011), and $C(Q)$ is the correction factor due to high gas flow rate (Chen et al. 2016 and 2017). For an idealised free-field and bubble-free propagation path, the column matrix of bubble generation rate, $\varphi(R_{0,n})$, is then obtained by inverting the spectrum matrix in Eq. 3. Those equations provide a correlation between the power spectral density of bubble acoustic emission, $S(\omega)$, and the bubble generation rate/size distribution. The total flow rate of the system, Q, can be then obtained by summing the bubble generation rate distribution.

At a high gas-flux rate, a plume of large dimension consisting of many bubbles is formed. When an incident sound wave passes through this large bubble plume, the bubbles of natural frequency close to the frequency of the incident wave will extract energy from the incident wave very efficiently by scattering and absorption, leading to the attenuation of the sound wave. This is the so-called 'sound screening' effect. If the bubble creation occurs within a bubble plume, the acoustic emission received at a distance will also be attenuated. If this effect is not properly accounted for, the use of Eq. 3 based on the measured acoustic spectrum would under-estimate the number of the bubbles generated. It is therefore important to include accurate descriptions of significant departures from the idealized free-field bubble-free propagation theory of Eq. 3. An accurate estimation of the bubble generation rate and size distribution of a turbulent bubble plume using a passive acoustic technique depends on a good model for the magnitude of the sound emitted through a realistic sound propagation path by formation of each individual bubble, and an accurate free-field sound measurement. The latter is crucial when the technique is applied to an enclosure, e.g. for bubble generation in a water tank.

The effects of turbulent flow on the magnitude of bubble formation sound have been explored in Chen et al. (2016, 2017). Obtaining a free-field sound measurement in a confined space has been reported by Trinh et al. (2018). The effect of a turbulent bubble plume on the sound transmission and the effect of the bubble size on the magnitude of acoustic emission are taken into consideration in the following.

According to Deane and Stokes (2010), based on Commander and Prosperetti (1989), if the bubble creation is within a cylindrical bubble-plume then the power spectrum, including the sound screening effect, will be given by

$$P(\omega,\mathbf{r}) = \oiiint \int_{R_{0,min}}^{R_{0,max}} \varphi(R_0)|P(\omega,R_0)G(\omega,\mathbf{r})|^2 dR_0\, dV \tag{5}$$

where V is the volume of the plume. The corresponding Green's function is given by

$$G(\omega,\mathbf{r}) = \frac{e^{-\frac{f|\mathbf{r}-\mathbf{r}_r|}{L_e}}}{|\mathbf{r}-\mathbf{r}_r|}\,. \tag{6}$$

Here, f is the fraction of the sound propagation path $|\mathbf{r}-\mathbf{r}_r|$ that lies in the bubble-plume and $\mathbf{r}_r$ is the observation point. This model assumes that bubble formation sound decays exponentially with distance through the fraction of the path that lies within the bubble plume at a rate of $1/L_e$. The distance L_e, or e-folding length, is the distance over which a plane wave of specified frequency propagating through an unbounded plume decays in amplitude by the factor $1/e$. Deane and Stokes (2010) introduced a volume correction, $\beta(\omega)$, that will be referred to as the 'attenuation correction factor' in the following text, to account for the attenuation of the bubble formation sound by a cylindrical plume of bubbles in water. According to the definition, it is given as

$$\beta(\omega) = \frac{R_r^2}{V}\iiint |G(\omega,\mathbf{r})|^2\, d\mathbf{r} \tag{7}$$

where R_r is the radius of the observation point. Substituting Eq. 7 into Eq. 5 and taking the effect of the formed bubble size on the amplitude of acoustic emission into consideration as $F(R_0)$, leads to

$$P(\omega,\mathbf{r}) = \frac{V}{R_r^2}\int_{R_{0,min}}^{R_{0,max}} \beta(\omega)\varphi(R_0)|P(\omega,R_0)|^2 F(R_0) dR_0. \tag{8}$$

$F(R_0)$ is a filter-like function based on Deane and Stokes (2010). After some manipulation, the above equation becomes

$$\beta(\omega) = \frac{\phi^2}{2\pi\psi}\int_{\psi}^{-\psi}\int_0^1\int_0^{2\pi} \frac{e^{2f(\emptyset^2-2\alpha\emptyset cos(\theta)+\alpha^2+\gamma^2)\zeta^{-0.5}}}{(\emptyset^2-2\alpha\emptyset cos(\theta)+\alpha^2+\gamma^2)}\alpha d\theta d\alpha d\gamma, \tag{9}$$

where the observation location, x_r, and half-height of the plume, H_{plume}, and the e-folding length, L_e, are normalised by the radius of the bubble plume, R_{plume}, according to:

$$\phi = \frac{x_r}{R_{plume}}, \psi = \frac{H_{plume}}{R_{plume}}, \zeta = \frac{L_e}{R_{plume}}, \tag{10}$$

Term f is the a function of ϕ and γ. α and γ are non-dimensional cylindrical coordinates of r and z normalised by the bubble plume radius determined experimentally. The e-folding length is related to the extinction cross-section per unit volume , S_e, as $L_e = 1/S_e$, which is calculated as

$$S_e = \frac{2\pi^2 R^3 \Psi(R)}{\delta_{tot,R}} \tag{11}$$

$\delta_{tot,R}$ is the total damping coefficient that can be found in Leighton (1998), and $\Psi(R)$ is the bubble number per unit volume. Eq. 11 is based on the assumption that only bubbles of near-resonance size will dominate the scattering cross-section at any particular frequency.

The bubble plume dimension is obtained experimentally by using a Nikon D4 DSLR camera. A total of 400 images of the bubble plume over 400 seconds were averaged for each experimental condition. Sample images of the plume are shown in Fig. 1. As can be seen, it is reasonable to approximate them as being cylindrical to simplify the model. The mean radius as a function of the total gas flow rate was estimated based on the averaged images as

$$R_{plume} = 3.74 \times 10^{-7} Q^3 - 8.15 \times 10^{-5} Q^2 + 0.0085Q + 0.068; \qquad V = 2\pi R_{plume}^2 H_{plume} \tag{12}$$

Here *Q* is in litre/minute, *H* and *R* are in metre.

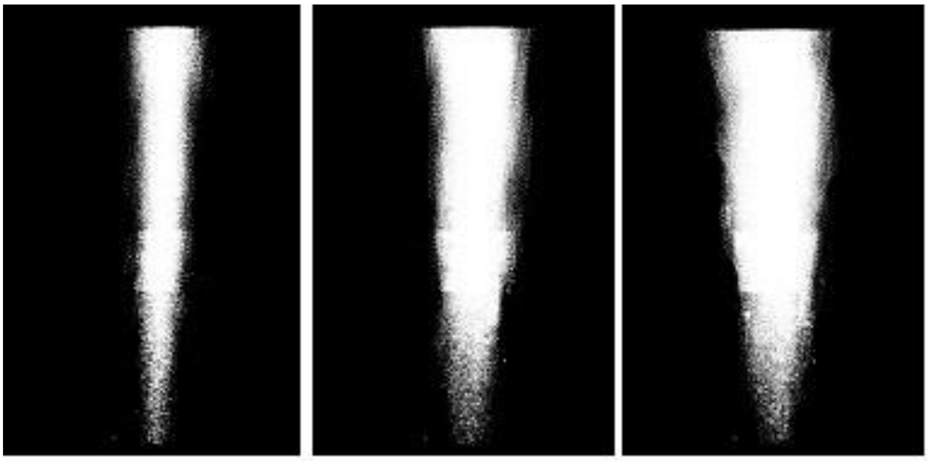

(a) 10 l/min (b) 30 l/min (c) 40 l/min

Figure 1. Shape of plumes at different flow rates

In this study, the correction derived to account for the effect of the high gas flow rate on the amplitude of bubble formation sound is shown in Fig 2, which decays approximately exponentially with the increase of the total gas flow rate. The detailed procedure to obtain this correction can be found in Chen et al. (2016, 2017).

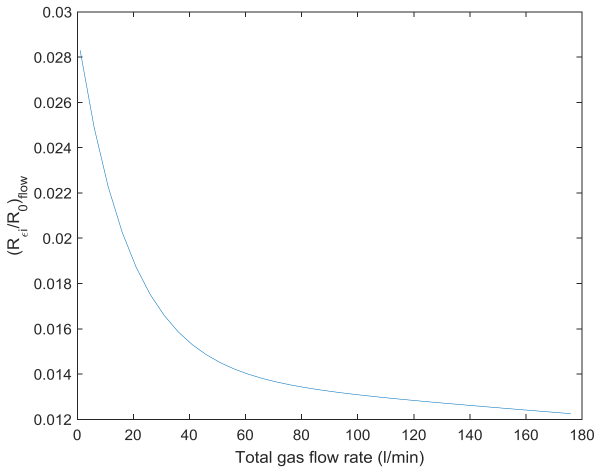

Figure 2 Correction $C(Q)$ as function of gas flow rate

The solution for the bubble generation rate using Eq. 3 becomes non-linear due to the inclusion of the effects of the sound screen, as to calculate the attenuation coefficient, S_e, the bubble number distribution or bubble number generation rate is required. Therefore an iterative method has to be used. The iteration starts by setting the correction β equal to one, and updating it when the new bubble generation rate and size distribution are available. The convergence criterion is based on the relative error defined as $(Q_n - Q_{n-1})/Q_{n-1}$ in which *n* is the iteration step. The solution flowchart is given in Figure 3.

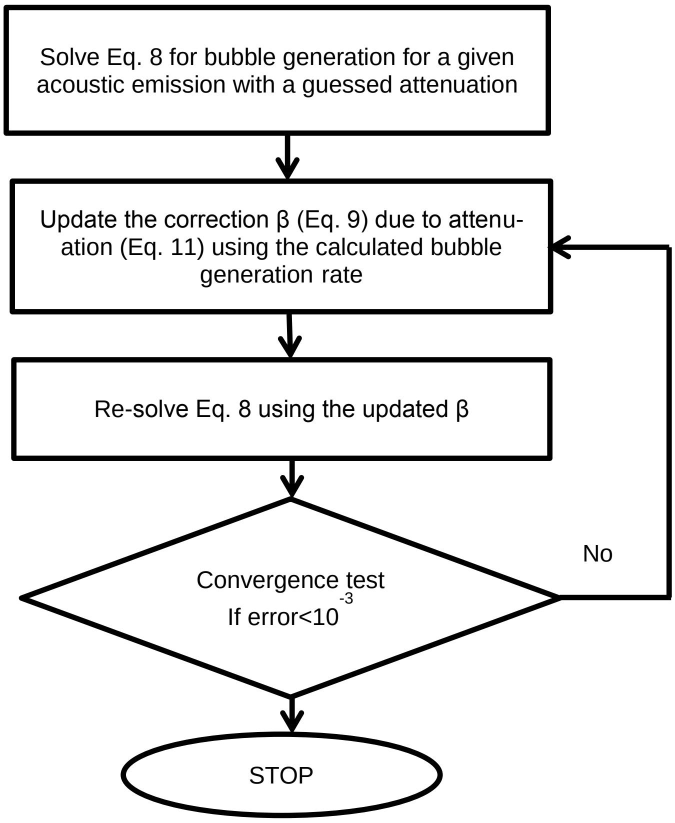

Figure 3 Solution flowchart

3 RESULTS AND DISCUSSIONS

The improved correction between the measured sound and bubble generation rate is applied to experiments involving gas discharged at different flow rates and with different nozzle sizes in different water tanks. Chen et al. (2016, 2017) measured the free-field bubble formation sound in a $10\text{m} \times 10\text{m} \times 6\text{m}$ water tank with gas discharge rates varying from 5 to 50 l/min through three circular nozzles of diameter 4 mm, 6 mm and 9 mm. Xu et al. (2013) measured the bubble sound in a $2\text{m} \times 2\text{m} \times 1\text{m}$ water tank at gas discharge rates of 163 l/min and 329.9 l/min through a nozzle of a diameter of 15.6 mm. The bubble generation rates under those conditions are predicted using the measured sound.

The predicted bubble generation rates per μm or size distributions at different flow rates, with the 9mm nozzle, and for $Q = 30$ l/min through the 4mm, 6mm and 9mm nozzles are shown in Figure 4a and 4b, respectively. It can be seen that an increase in gas flow rate results in an increase in the rate of bubble generation of all sizes, as expected, and that the nozzle size does affect the rate of bubble generation and the size distribution.

The estimated acoustic attenuation and the corresponding volume correction due to bubble plumes of different nozzles at 30 l/min are depicted in Figures 5a and 5b respectively. It can be seen that the acoustic attenuations are very low, but the size of the nozzle affects the acoustic attenuation. The large nozzle (9mm) results in higher acoustic attenuations at frequencies between 2000 to 8000 Hz because of an increase in bubble number at the radius range between 0.1mm to 0.4mm (see Figure 4b). It has been found that for the same nozzle, the acoustic attenuation increases with an increase in gas flow rate due to the increase in the number of bubbles formed as expected but it is very low due to the short transmission path. The results are not shown here.

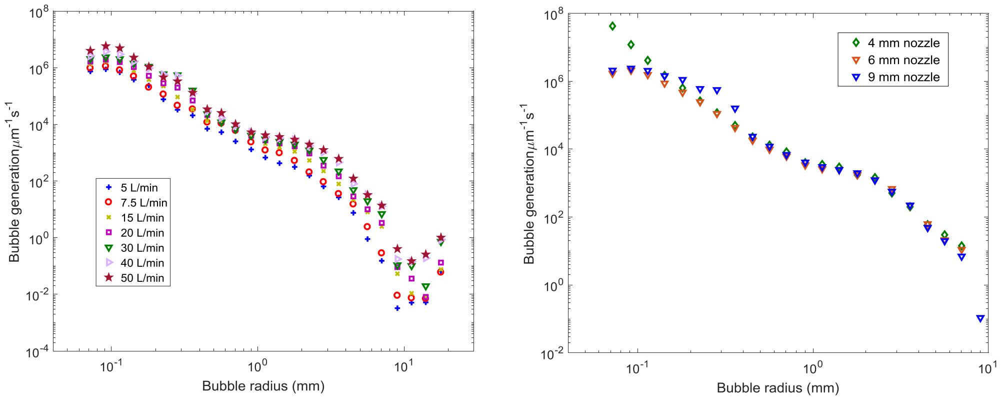

(a) Different flow rates for the 9mm nozzle (b) different nozzles for $Q = 30$ L/min

Figure 4 Bubble generation rates *D* at different flow rates and nozzles

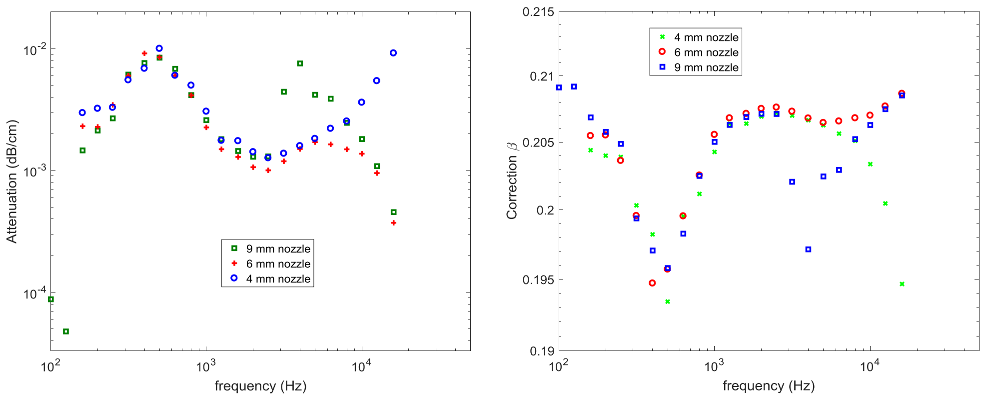

(a) Attenuation (b) volume correction

Figure 5 calculated attenuation and volume correction for different nozzles for $Q = 30$ L/min

Ideally the predicted bubble number distribution would be compared with a direct measurement. However, measuring size distribution accurately for a high gas flow rate using a typical optical technique, such as with a high speed camera, is not a trivial task. Therefore, in this paper, the accuracy of the improved correlation between the measured sound and bubble generation rate is demonstrated by comparing the predicted total gas flow rate to the measured value. The air flow rate was measured with a flow meter located on the top of the tank and held constant for each measurement. The comparison is illustrated in Figure 6 by the relative error. The errors vary by around $\pm 30\%$ for most measurements for the 4 mm, 6 mm and 9 mm nozzles, except at the lowest flow rates of the 4 mm nozzle. The errors when using the two measurements of Xu et.al (2013) have been found to be approximately 86% and 80%. As the sound measured by Xu et al. (2013) was not free-field, and included the reverberation of the tank walls, the predicted gas flow discharge rates are in reasonable agreement with the measurements. However, the model can be further improved if the nozzle dimension is introduced explicitly.

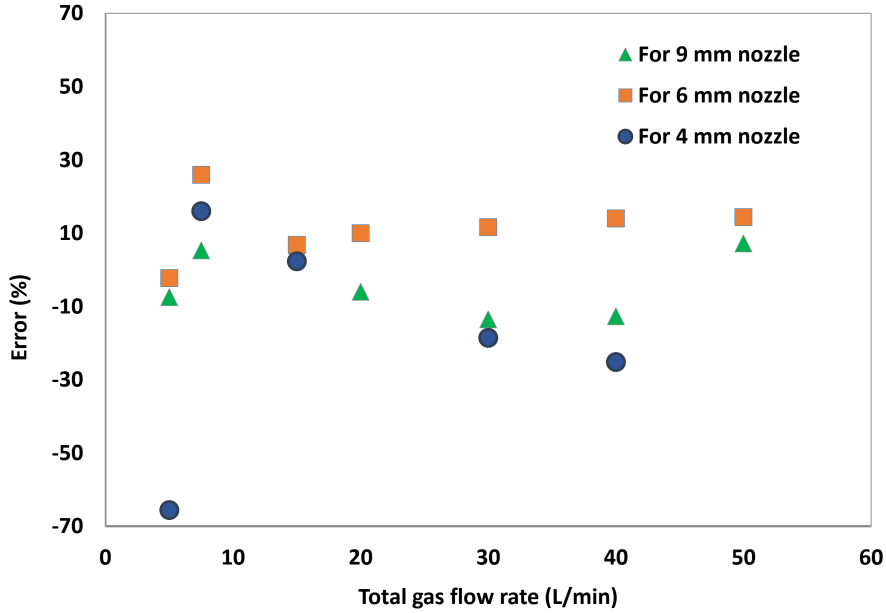

Figure 6 Relative differences between the predicted and measured gas flow rate

4 CONCLUSIONS

An improved iterative correlation between measured sound and bubble generation rate and size distribution has been presented. The correlation accounts for the effect of the bubble plume on bubble formation sound transmission and the effect of formed bubble size on the sound. The predicted bubble generation rates for a given acoustic emission compare well with experimental measurements. This demonstrates that the improved correlation is capable of relating measured sound to the bubble generation rate. It has been found that the bubble generation rate increases with an increase of gas flow rate as expected, and the nozzle size affects the bubble size distribution. These results also confirm our previous finding that the magnitude of bubble formation sound indeed decreases with an increase of gas flow rate due to the increasing influence of the induced turbulent flow on the bubble formation dynamics.

It has been found that, at the flow rates studied, the effect of the bubble plume on the sound transmission is weak. That is sound attenuations through the bubble plume are low, which justify the choice of the simple model used. However, it is important to include this effect if a passive acoustic technique is used.

In the current model framework, the effect of gas flow rate on the amplitude of the bubble generation sound is not included in the solution loop because it is a primary input for the applications of interest. Therefore, the current model is applicable to where the bubble generation rate and size distribution are of the primary interest and the overall flow rate is known.

ACKNOWLEDGEMENTS

The author would like to express sincere appreciation to Professors Leighton and White for their valuable comments and suggestions in improving the model. The author would also like to thank Mr Trinh, Dr Yang and Dr Mohanangam for their help in measuring the plume size.

REFERENCES

Berges, B. J. P., Leighton, T. G. and White, P. R. 2015. 'Passive acoustic quantification of gas fluxes during controlled gas release experiments', International Journal of Greenhouse Gas Control, 38, 64–79(doi:10.1016/j.ijggc.2015.02.008).

Brooks, I.M., et al. 2009, 'Physical Exchanges at the Air Sea Interface: UK SOLAS Field Measurements', Bulletin of the American Meteorological Society, 90, 629–644 doi: 10.1175/2008BAMS2578.

Bok, K., and Suk, W. (2001). ‘Acoustic bubble counting technique using sound speed 423 extracted from sound attenuation,’ IEEE J. Oceanic Engineering 26(1), 125-130.

Chen L., Leighton T.G. and White, P.R. 2017. ‘Study of Bubble Formation Dynamics Based On Associated Acoustic Radiation’, In Proceedings of 24th International Congress on Sound and Vibration, 23-27 July, London.

Chen L., Trinh V., Yang, W. and Mohanangam, K. 2016. ‘Prediction of bubble generation based on acoustic emission’, Acoustics Australia, DOI 10.1007/s40857-016-0054-7.

Commander, K.W. and Prosperetti, A. (1989), ‘Linear pressure waves in bubbly liquids: comparison between theory and experiments’, J. Acoust. Soc. Am. 85, 732-746.

Deane, G.B. and Stokes, M. D. 2008. ‘The acoustic excitation of air bubbles fragmenting in sheared flow’. Journal of the Acoustical Society of America 102, 2671–2689.Deane, G. B., and Stokes, M. D. (2010). “Model calculations of the underwater noise of
445 breaking waves and comparison with experiment," J. Acoust. Soc. Am. 127(6), 3394-3410.

Gavigan, J.J., Watson, E.E. and King III,W.F.1974. ‘Noise generation by gas jets in a turbulent wake’, Journal of the Acoustical Society of America, 56 (4), 1094–1099.

Leighton, T.G. and Walton, A.J. 1987. ‘An experimental study of the sound emitted from gas bubbles in a liquid’. European Journal of Physics. 898–104.

Longuet-Higgins, M. 1990. ‘Bubble noise spectra’. Journal of the Acoustical Society of America. 87(2),652–661.

Pandit, A.B., Varley, J., Thorp, R.B. and Davidson, J.F. 1992. ‘Measurement of bubble size distribution: an acoustic technique’, Chemical Engineering Science, 47 (5), 1079–1089.

Strasberg, M. 1956. ‘Gas bubbles as sources of sound in liquids’. Journal of the Acoustical Society of America, 28 20–26.

Trinh, V, Chen L. and Forrest, J. 2018, ‘Free-field acoustic source levels from measurements conducted in a water tank’, Proceedings of Acoustics 2018, 7-9, Nov. Adelaide, Australia

Xu, W., Lai, Z., Wu, D. and Wang, L. 2013, ‘Acoustic emission characteristics of underwater gas jet from a horizontal exhaust nozzle’, Applied Acoustics, 74 845-849.